

# ***Analysis of Organoiodide Adsorption Mechanisms***

**Nuclear Technology  
Research and Development**

***Prepared for  
US Department of Energy  
Material Recovery and Waste Form  
Development Campaign***

***A. T. Greaney and S. H. Bruffey***

***Oak Ridge National Laboratory  
30 April 2021  
ORNL/SPR-2021/2003***





**DISCLAIMER**

This information was prepared as an account of work sponsored by an agency of the U.S. Government. Neither the U.S. Government nor any agency thereof, nor any of their employees, makes any warranty, expressed or implied, or assumes any legal liability or responsibility for the accuracy, completeness, or usefulness, of any information, apparatus, product, or process disclosed, or represents that its use would not infringe privately owned rights. References herein to any specific commercial product, process, or service by trade name, trade mark, manufacturer, or otherwise, does not necessarily constitute or imply its endorsement, recommendation, or favoring by the U.S. Government or any agency thereof. The views and opinions of authors expressed herein do not necessarily state or reflect those of the U.S. Government or any agency thereof.

## SUMMARY

If the United States were to engage in the reprocessing of used nuclear fuel, radioactive iodine must be removed from multiple plant off-gas streams to comply with governing regulations. One of these streams is the vessel off-gas (VOG), which arises from the separations process and is expected to contain iodine in primarily organic iodine forms and at parts-per-billion concentrations. The relative lack of knowledge surrounding organic iodine removal from the VOG prompted the US Department of Energy's Office of Nuclear Energy to initiate experimental efforts targeted at understanding organic iodide removal from prototypic VOG streams. At Oak Ridge National Laboratory (ORNL), this effort has focused on developing a comprehensive understanding of iodine removal from VOG streams by using silver-based sorbents. An important aspect of this testing is developing an understanding of how the sorption of methyl iodide ( $\text{CH}_3\text{I}$ ), the most studied organic iodide species to date, compares with the sorption of other volatile organic iodide species potentially present in the VOG.

The work presented here reflects initial testing that will continue to be developed, and final results will be incorporated into an end-of-year report that details a multiyear testing campaign designed to understand iodine mitigation from VOG streams. The goal of these experiments was to determine whether similar reaction pathways govern both  $\text{CH}_3\text{I}$  and iodobutane ( $\text{C}_4\text{H}_9\text{I}$ ) sorption onto silver mordenite (AgZ), a common silver-based iodine sorbent. More specifically, the authors hypothesized that the sorption of  $\text{C}_4\text{H}_9\text{I}$  by AgZ will result in the formation of butanol ( $\text{C}_4\text{H}_9\text{OH}$ ). Effluent monitoring of  $\text{CH}_3\text{I}$  sorption testing has confirmed methanol production, but analogous monitoring of effluents from  $\text{C}_4\text{H}_9\text{I}$  sorption studies has not been performed.

A series of tests was completed to test this hypothesis with the aim of detecting  $\text{C}_4\text{H}_9\text{OH}$  downstream of the AgZ bed. Test conditions varied the bed depth, gas stream humidity, and bed temperature post sorption. The effluent gas stream downstream of the AgZ bed was sampled by using gas-tight syringes, and these samples were analyzed by a gas chromatograph coupled to a mass spectrometer.

Thin bed  $\text{C}_4\text{H}_9\text{I}$  tests conducted at  $-65$  and  $0^\circ\text{C}$  dew points did not result in  $\text{C}_4\text{H}_9\text{OH}$  detection in the effluent. This suggests that the sorption mechanism and subsequent reactions could be different from those observed for  $\text{CH}_3\text{I}$ . The sorption testing continues; additional results will be included in final end-of-year report and will increase the fundamental understanding of organic iodide sorption by AgZ from VOG streams.

## CONTENTS

SUMMARY .....	ii
FIGURES .....	iv
TABLES .....	iv
ACRONYMS .....	v
1. INTRODUCTION .....	1
2. BACKGROUND .....	2
3. METHODS .....	3
3.1 Experimental Methods .....	3
3.2 Analytical Methods .....	5
3.3 Completed Tests .....	5
4. OBSERVATIONS .....	6
4.1 SM-2 and SM-3: C <sub>4</sub> H <sub>9</sub> I Deep Bed Tests .....	6
4.2 SM-4 and SM-5: C <sub>4</sub> H <sub>9</sub> I Thin Bed Tests .....	7
4.3 SM-6 and SM-7: C <sub>4</sub> H <sub>9</sub> I and C <sub>4</sub> H <sub>9</sub> OH Burn-Off Tests .....	7
4.4 SM-8: CH <sub>3</sub> I Loading and Burn-Off .....	9
5. CONCLUSIONS AND FUTURE TESTS .....	10
6. REFERENCES .....	10

## FIGURES

Figure 1. Diagram of experimental setup. ....	4
Figure 2. Chromatographs showing examples of calibration standards analyzed. The y-axis is the counts (not to scale between figures), and the x-axis is time. Purple is 100 ppm, black is 50 ppm, green is 10 ppm, and orange is 1 ppm. ....	5
Figure 3. Chromatograph showing a syringe background sample (black, ~6 ppm) and an effluent sample from the humid SM-3 test (blue, ~12 ppm). C <sub>4</sub> H <sub>9</sub> OH (peak at 10 min) is present in both samples, suggesting that contamination from the syringe could account for C <sub>4</sub> H <sub>9</sub> OH signals observed in the effluents of SM-2 and SM-3. ....	7
Figure 4. Loading rates of CH <sub>3</sub> I and C <sub>4</sub> H <sub>9</sub> I on thin bed tests recorded by TGA. ....	9

## TABLES

Table 1: Proposed CH <sub>3</sub> I sorption pathways. <i>Synthesized from Scheele et al. (1983) and Huve et al. (2018)</i> . ....	2
Table 2: LODs and LOQs for monitored species. ....	5
Table 3. Matrix of test conditions. ....	6
Table 4. Results of C <sub>4</sub> H <sub>9</sub> I and C <sub>4</sub> H <sub>9</sub> OH burn-off tests. ....	8

## ACRONYMS

AgI	silver iodide
AgZ	silver mordenite
BDL	below limit of detection
BQL	below limit of quantification
C <sub>2</sub> H <sub>6</sub>	ethane
CH <sub>3</sub> I	methyl iodide
CH <sub>3</sub> OH	methanol
C <sub>4</sub> H <sub>9</sub> I	iodobutane
C <sub>4</sub> H <sub>9</sub> OH	butanol
C <sub>12</sub> H <sub>25</sub> I	iodododecane
DF	decontamination factor
DME	DME
DOG	dissolver off-gas
GC	gas chromatography
GC-MS	gas chromatography-mass spectrometry
I <sub>2</sub>	elemental iodine
INL	Idaho National Laboratory
LOD	limit of detection
LOQ	limit of quantification
MS	mass spectrometer
ORNL	Oak Ridge National Laboratory
SPME	solid phase microextraction
TGA	thermogravimetric analyzer
VOG	vessel off-gas





# ANALYSIS OF ORGANOIODIDE ADSORPTION MECHANISMS

## 1. INTRODUCTION

The aqueous reprocessing of used nuclear fuel releases four key volatile radionuclides— $^3\text{H}$ ,  $^{14}\text{C}$ ,  $^{85}\text{Kr}$ , and  $^{129}\text{I}$ —from the used fuel into the off-gas streams of a reprocessing facility. Off-gas streams, which typically converge to one environmental discharge point, are treated within the facility to remove volatile radionuclides. Analysis shows that of these four volatile elements, iodine will require the highest level of removal to comply with US Environmental Protection Agency regulations (Jubin et al. 2012). An evaluation was conducted that assessed the practical impact of these regulations, and it found that an overall plant decontamination factor (DF)<sup>a</sup> of 1,000 is likely the minimum required iodine abatement efficiency (Jubin et al. 2017). Depending on the specifics of the reprocessing facility and reprocessed fuel, the required DF could be as high as 8,000.

Iodine is released during multiple unit operations within the plant and can be found in gas streams such as the shear off-gas, dissolver off-gas (DOG), solvent extraction vessel off-gas (VOG), and waste solidification off-gas. An analysis of the distribution of iodine between aqueous separations unit operations found that 95–99% of total iodine release to the off-gas occurs during dissolution, releasing iodine into the DOG, and also found that much of the balance of the iodine is released during solvent extraction, releasing the iodine into the VOG (Jubin et al. 2013). To achieve DFs greater than 1,000, the treatment of the plant off-gas streams must include, at minimum, the treatment of both DOG and VOG.

Removing iodine from the DOG has been the subject of substantial research and development in recent years. Iodine is primarily present in the DOG as elemental iodine ( $\text{I}_2$ ) and is typically removed by using silver-based sorbent materials or aqueous caustic scrubbing. Interest in removing iodine from the VOG has also recently increased, and a 2015 analysis showed that the iodine speciation in the VOG primarily comprises organic alkyl iodides and that abatement technology for organic iodides is not well developed (Bruffey et al. 2015). Furthermore, the concentration of iodine in the VOG (parts per billion by volume levels) is substantially lower than that of the DOG (parts per million by volume levels), and the characteristics of the two gas streams differ in total flow rate, volume, and composition.

Because iodine abatement within the VOG might be a critical requirement for an eventual reprocessing facility, the relative lack of knowledge that surrounds iodine removal from the VOG prompted the US Department of Energy's Office of Nuclear Energy to initiate experimental efforts targeted at understanding organic iodide removal from prototypic VOG streams. At Oak Ridge National Laboratory (ORNL), this effort has focused on developing a comprehensive understanding of iodine removal from VOG streams by using silver-based sorbents (Jubin et al. 2017, Jubin et al. 2018, Bruffey et al. 2018). Variables such as the mass transfer zone of the sorbent bed, gas velocity, sorbate concentration, and sorbate speciation are being explored to determine their effects on iodine removal from VOG streams. One important aspect of this testing is developing an understanding of how the sorption of methyl iodide ( $\text{CH}_3\text{I}$ ), the most studied organic iodide species to date, compares with the sorption of other volatile organic iodide species potentially present in the VOG. Tests at ORNL and Idaho National Laboratory (INL) have investigated the sorption of the longer chain alkyl iodides iodobutane ( $\text{C}_4\text{H}_9\text{I}$ ) and iodododecane ( $\text{C}_{12}\text{H}_{25}\text{I}$ ) to understand how iodine speciation might affect iodine sorption by silver-based sorbents (Bruffey et al. 2019).

The experiments described in this report were conducted as part of the larger effort to understand organic iodine removal from the VOG. This work aimed to incorporate effluent monitoring into ORNL testing to

---

<sup>a</sup>  $\text{DF} = \frac{\text{concentration of radionuclide in a control device inlet gas}}{\text{concentration of radionuclide in a control device outlet gas}}$

provide more insight into the reaction pathways of  $C_4H_9I$  sorption by silver mordenite (AgZ), a common silver-based zeolite mineral sorbent. Much of the testing at ORNL to date has been limited to continuous weight measurements via a custom thermogravimetric analyzer (TGA) and posttest sorbent analysis for total iodine content. These measurements provide insight into loading rates and sorbent iodine capacity values across a range of operating conditions, but they cannot provide insight into the specific sorption mechanisms that drive sorption rates or capacities.

The experiments described in this report extend the current understanding of organic iodide sorption by zeolites. The literature reflects knowledge of the reaction pathways that govern  $CH_3I$  sorption, but it does not address whether similar pathways can be validated for other iodine-bearing species. This work reflects initial testing that will continue to be developed, and an end-of-year report will detail the final results of the multiyear testing campaign designed to understand iodine mitigation from VOG streams.

## 2. BACKGROUND

There is a dense body of literature surrounding the sorption of organic iodides, primarily  $CH_3I$ , by silver-based sorbents, as documented in a review article by Huve et al. (2018). A formal review of this information is outside the scope of this report, but relevant portions are discussed in this section to provide an understanding of the test aims and experimental approach.

Some of the earliest documentation of potential sorption pathways for  $CH_3I$  by AgZ is found in Scheele et al. (1983). Scheele et al. tabulated the free energies of many relevant reactions, including those of  $I_2$  sorption by AgZ with and without the presence of  $NO_x$  gas in the initial feed stream. Huve et al. (2018) provides a more condensed list of potentially applicable reactions. Reactions from these papers are provided in Table 1, and the free energies are updated in this document by using the thermodynamic calculation software HSC Chemistry Version 9 (Outotec 2018) for three temperatures. Studies also show that the sorption of  $CH_3I$  by AgZ is catalyzed by the zeolite surface itself (Nenoff et al. 2014). This is reflected in Table 1 by the inclusion of Reaction 0, a decomposition of  $CH_3I$  to a  $CH_3$ -zeolite complex. The  $CH_3$ -zeolite complex can then continue to react to form methanol ( $CH_3OH$ ) or other organic compounds. Catalysis of  $CH_3I$  by the zeolite surface might facilitate some or all of equations 1–6 in Table 1.

**Table 1:** Proposed  $CH_3I$  sorption pathways. *Synthesized from Scheele et al. (1983) and Huve et al. (2018).*

Equation	Proposed sorption reactions	$\Delta G_{\text{reaction}}$ (kcal)		
		300 K	400 K	500 K
0	$CH_3I + \text{Ag-zeolite} \leftrightarrow CH_3\text{-zeolite} + AgI$	Not tabulated		
1	$2Ag + 2CH_3I(g) \rightarrow 2AgI + C_2H_6(g)$	-46.9	-43.9	-41.5
2	$Ag^0 + CH_3I(g) + H_2O(g) \rightarrow AgI + CH_3OH(g) + 1/2H_2$	-7.6	-4.6	-2.4
3	$Ag + CH_3I(g) + CH_3OH \rightarrow AgI + CH_3OCH_3(g) + 1/2H_2$	-15.7	-11.7	-8.5
4	$Ag^+(aq) + CH_3I(g) + H_2O(g) \rightarrow AgI + CH_3OH(g) + H^+(aq)$	-22.2	-18.3	-14.7
5	$7NO + 2CH_3I(g) \rightarrow I_2(g) + 2CO_2 + 3H_2O(g) + 7/2N_2$	-500.4	-499.1	-497.8
6	$7NO_2(g) + 4CH_3I(g) \rightarrow I_2(g) + 4CO_2 + 6H_2O(g) + 7/2N_2$	-398.4	-404.4	-410.5

In Reactions 1–4, the iodine-bearing adsorbed species is solid silver iodide (AgI), which can be present in multiple crystalline forms, depending on specific sorption conditions (Chapman et al. 2010). Beyond AgI production, several key organic byproducts could also be present, depending on the reaction pathway. Reaction 1 produces ethane (C<sub>2</sub>H<sub>6</sub>), Reaction 2 produces CH<sub>3</sub>OH, and Reaction 3 provides a pathway for the CH<sub>3</sub>OH to further react and form dimethyl ether (DME).

In Reactions 5 and 6, AgI is not identified as the product, and the NO (Reaction 5) or NO<sub>2</sub> (Reaction 6) reactant serves to facilitate the production of free I<sub>2</sub>. This I<sub>2</sub> could be assumed to continue to react and adsorb onto the AgZ, indicating that more complex reaction pathways will be present in NO<sub>x</sub>-bearing gas streams.

These proposed reactions have been supported through the observation of the suggested byproducts in the gaseous effluent streams of CH<sub>3</sub>I sorption experiments. INL has verified the presence of CH<sub>3</sub>OH and DME in the effluent streams of CH<sub>3</sub>I/AgZ sorption experiments (Soelberg and Watson 2016), validating Reactions 2 and 3. Chebbi et al. (2016) also reported CH<sub>3</sub>OH and DME in the effluents of similar sorption testing.

Additional studies have been added to the literature surrounding the fundamental mechanisms and characteristics of CH<sub>3</sub>I sorption by AgZ or other zeolites (Azambre et al. 2017, Chebbi et al. 2017, Huve et al. 2018, Tang et al. 2020, Chebbi et al. 2021). One remaining question relates to the role of water in the CH<sub>3</sub>I/AgZ sorption reaction. Chebbi et al. (2021) describes some of the published conflicting studies on the role of water in the sorption of CH<sub>3</sub>I by AgZ. Recent studies by ORNL confirm that water plays less of a role in CH<sub>3</sub>I sorption than initially thought, despite a significant difference in observed loading rates, depending on whether water is present in the gas feed stream. Greaney et al. (2020) found no statistical difference observed in the loading capacity of AgZ for CH<sub>3</sub>I from dry and humid gas streams. The findings of Greaney et al. (2020) broadly align with the findings of Chebbi et al. (2021).

The work described here focuses on the sorption of C<sub>4</sub>H<sub>9</sub>I by AgZ and attempts to determine whether the sorption reactions that govern CH<sub>3</sub>I can be translated to the sorption of C<sub>4</sub>H<sub>9</sub>I. Specifically, the authors hypothesized that the sorption of C<sub>4</sub>H<sub>9</sub>I by AgZ will result in the formation of butanol (C<sub>4</sub>H<sub>9</sub>OH). A series of thin and deep bed sorption tests were performed, and the gaseous effluents were analyzed by gas chromatography (GC) coupled to a mass spectrometer (MS). Given the uncertainties surrounding the impact of water on organic iodine sorption, experiments were performed by using dry and humidified feed gas streams. Future reports will use these data to provide insights into organic iodide removal from VOG streams across a spectrum of fundamental and applied scales.

### 3. METHODS

Experimental methods included exposing thin and deep beds of reduced AgZ to dry and humid iodine-bearing feed streams. Effluent monitoring of the sorbate (C<sub>4</sub>H<sub>9</sub>I) and potential organic product (C<sub>4</sub>H<sub>9</sub>OH) was performed by gas chromatography-mass spectrometry (GC-MS). Validating experimental methodology included some testing with CH<sub>3</sub>I as the sorbate, and in these tests, CH<sub>3</sub>I and CH<sub>3</sub>OH were monitored. Although DME is also known to be produced in the sorption of CH<sub>3</sub>I by AgZ, its release is near simultaneous with CH<sub>3</sub>OH, and it is of lower abundance (Chebbi et al. 2021). Thus, monitoring for CH<sub>3</sub>OH or C<sub>4</sub>H<sub>9</sub>OH was judged sufficient to confirm reaction pathways.

#### 3.1 Experimental Methods

AgZ was obtained from molecular products in an engineered pelletized form (Ionex-Type Ag 900 E16). It contains 11.9% silver by weight and has a 0.16 cm pellet diameter. Before use in testing, the sorbent material was dried at 270°C under flowing argon gas for 3 days. It was then reduced by 10 day exposure to a flowing H<sub>2</sub>-N<sub>2</sub> (4–96%) blend gas at 270°C.

A test system was designed so that two beds could be loaded simultaneously and their effluents could be sampled for GC-MS analysis (Figure 1). Columns with 2.73 in. internal diameter were used, and the flow rate was kept constant at 3.94 LPM. One column received humid air or dry air, and the second column received dry air. All sorbent loading was conducted at 150°C, and the burn-off temperatures of two tests reached 225°C. Nitrogen-sparged bubblers were used to generate the organic species of interest (i.e., CH<sub>3</sub>I, C<sub>4</sub>H<sub>9</sub>I, or C<sub>4</sub>H<sub>9</sub>OH). The inlet concentrations of the monitored products were verified through GC-MS analysis.

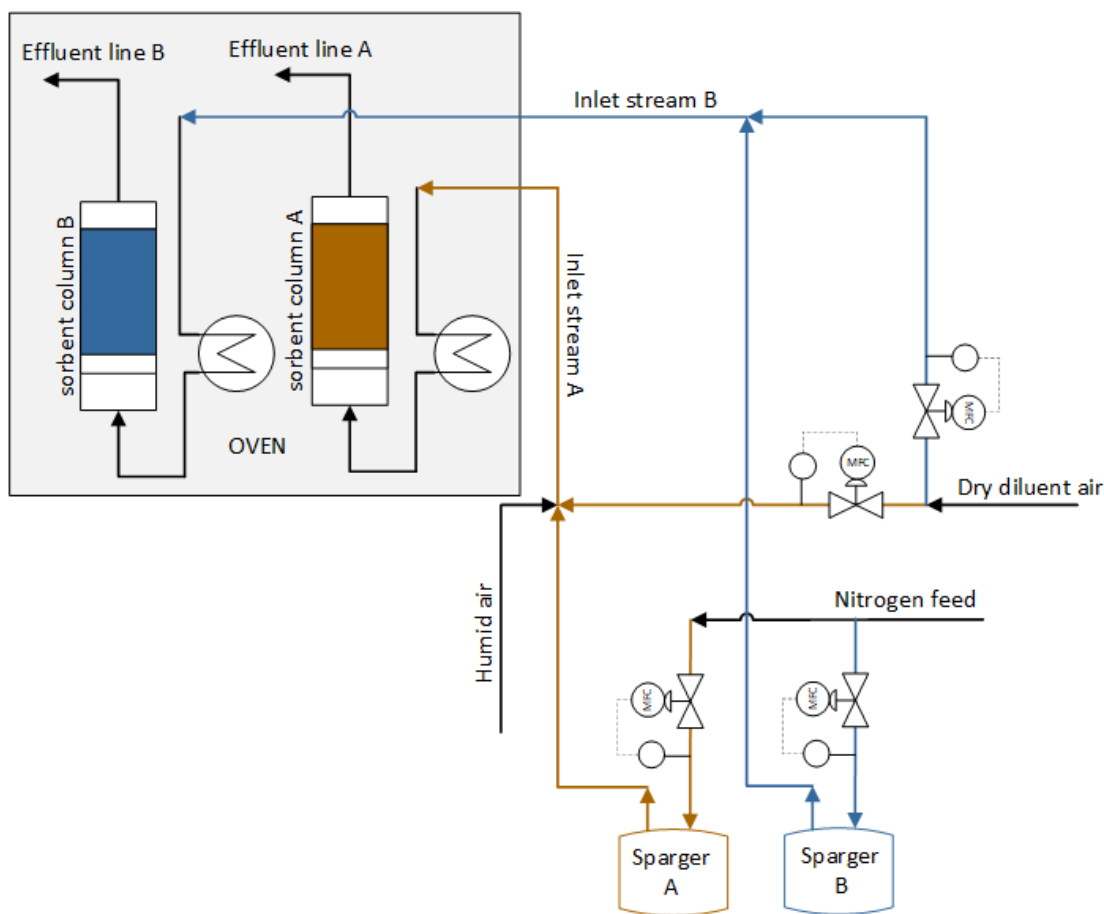


**Figure 1.** Diagram of experimental setup.

Multiple downstream sampling systems were tested for GC-MS analysis, including solid phase microextraction (SPME) fibers, capturing the effluent in flow-through gas-tight sampling vials and directly sampling the effluent with a gas-tight syringe. The SPME fibers were difficult to clean, which resulted in carryover between samples. The flow-through sampling vial resulted in imprecise data when it was used with one concentration gas stream. The most accurate and precise sampling method was determined to be the direct sampling of the effluent by using headspace syringes.

### 3.2 Analytical Methods

Effluent samples were analyzed on an Agilent 8890-5977B GC-MS with a 30 m DB-624-UI ultra-inert capillary column. The GC method was designed to capture iodoalkanes ranging from methyl to dodecyl iodide. The inlet temperature remains at 250°C while the column temperature starts at 30°C for 5 minutes before ramping to 220°C at a rate of 10°C/minute before holding at 220°C for 6 minutes. Helium is used as the carrier gas with a constant flow rate of 1.2 ml/min. The column effluent is analyzed on a single-quad mass spectrometer and the data are analyzed using the Agilent MassHunter software. Manual injections were of 200 µl sample volumes were done with gas-tight syringes. Methanol is detected on the chromatograph at 3 min, CH<sub>3</sub>I is detected at 4.5 min, C<sub>4</sub>H<sub>9</sub>OH is detected at 10.1 min, and C<sub>4</sub>H<sub>9</sub>I is detected at 13.2 min (Figure 2). An additional ramp temperature of 30 min to 220°C is included to ensure that C<sub>4</sub>H<sub>9</sub>OH fully burns off the column and is not carried over from sample to sample. Column and syringe backgrounds were analyzed at least once daily (often multiple times a day) by injecting 200 µl of room air into the GC-MS and running the aforementioned method.

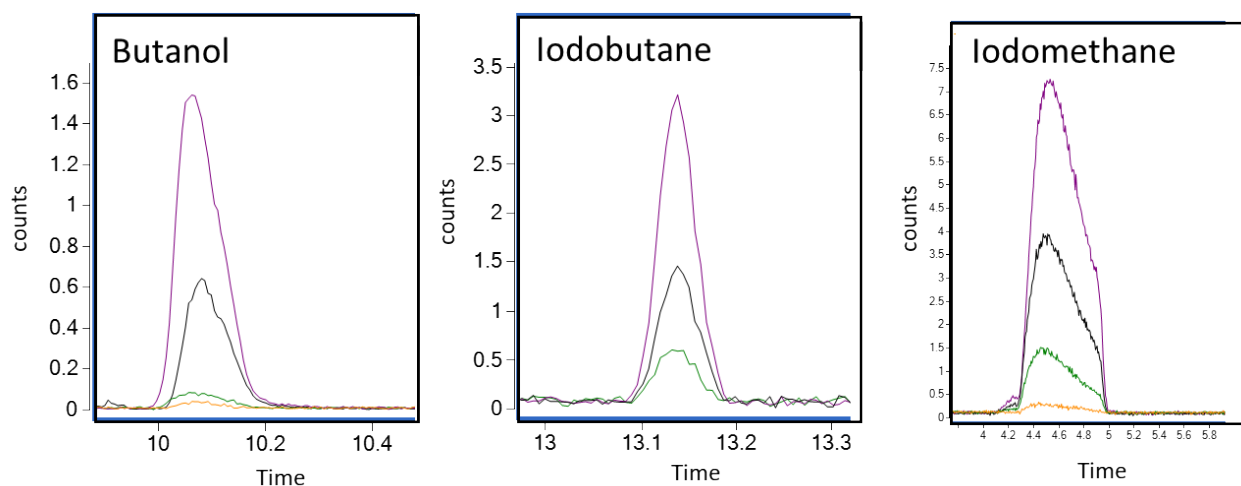


**Figure 2.** Chromatographs showing examples of calibration standards analyzed. The y-axis is the counts (not to scale between figures), and the x-axis is time. Purple is 100 ppm, black is 50 ppm, green is 10 ppm, and orange is 1 ppm.

Gas-phase calibration standards were created by using the same sampling methods as the experiments. Standards were created at 1, 10, 50, and 100 ppm. Peak areas integrated by the Agilent MassHunter software are used for quantification. Limits of detection (LODs) and limits of quantification (LOQs) were determined for each species using chromatograph baseline statistics and regression statistics from the calibration curve generated by the standards (Table 2). For reference, the vapor pressures of each compound are also included in Table 2. A 1 ppm standard was not analyzed for iodobutane. Iodomethane does not form a gaussian peak in the chromatograph, possibly due to effects of the compound interacting with the column. This peak broadening is routinely observed for iodomethane across experiments.

**Table 2:** LODs and LOQs for monitored species.

Species	LOD (ppm)	LOQ (ppm)	Vapor pressure (mmHg)
CH <sub>3</sub> I	0.06	0.13 ± 0.06	400 (20°C)
CH <sub>3</sub> OH	Not determined	Not determined	90 (25°C)
C <sub>4</sub> H <sub>9</sub> I	1	12 ± 1	0.138 (25°C)
C <sub>4</sub> H <sub>9</sub> OH	3	4 ± 1	4.35 (20°C)

### 3.3 Completed Tests

Seven tests are reported here, and a summary of test conditions is shown in Table 3; more detailed information is provided in Section 4.

**Table 3.** Matrix of test conditions.

SM test #	Species	Inlet conc. (ppm)	Sorbent	Temp. (°C)	Dew point (°C)	Carrier gas	Bed height (in.)	Bed Mass (g)
FY21-SM-2	C <sub>4</sub> H <sub>9</sub> I	20	Ag <sup>0</sup> Z	150	-70	Air	2	45
FY21-SM-3	C <sub>4</sub> H <sub>9</sub> I	20	Ag <sup>0</sup> Z	150	10	Air	2	45
FY21-SM-4	C <sub>4</sub> H <sub>9</sub> I	50	Ag <sup>0</sup> Z	150	-70	Air	1	18
FY21-SM-5	C <sub>4</sub> H <sub>9</sub> I	50	Ag <sup>0</sup> Z	150	0	Air	1	18
FY21-SM-6	C <sub>4</sub> H <sub>9</sub> I	50	Ag <sup>0</sup> Z	150	0	Air	0.25	4
FY21-SM-7	C <sub>4</sub> H <sub>9</sub> OH	50	Ag <sup>0</sup> Z	150	-70	Air	0.25	4
FY21-SM-8	CH <sub>3</sub> I	50	Ag <sup>0</sup> Z	150	10	Air	0.3	6

## 4. OBSERVATIONS

### 4.1 SM-2 and SM-3: C<sub>4</sub>H<sub>9</sub>I Deep Bed Tests

Initial tests to evaluate whether C<sub>4</sub>H<sub>9</sub>OH formed during sorption were conducted in deep sorbent beds (~45 g of AgZ in 2 in. deep bed). One dry test (SM-2) was conducted at 150°C, -70°C dew point, and 20 ppm C<sub>4</sub>H<sub>9</sub>I in air, and one humid test (SM-3) was conducted at 150°C, 10°C dew point, and 20 ppm C<sub>4</sub>H<sub>9</sub>I in air. The dry test ran for 12 days, and the humid test ran for 10 days, allowing portions of the sorbent beds to approach iodine loadings near capacity. The effluent was sampled for GC-MS analysis multiple times on the first day and then daily thereafter. Neither test resulted in detectable C<sub>4</sub>H<sub>9</sub>I breakthrough of the 2 in. deep bed.

The results of these tests were inconclusive. A transient C<sub>4</sub>H<sub>9</sub>OH peak and a cyclobutanol peak were detected in chromatographs from the wet and dry tests. A C<sub>4</sub>H<sub>9</sub>OH peak was present at the 46 h sample and 96 h sample but was absent from the 69 h sample. However, further analysis of the GC column and syringe background found that the observed C<sub>4</sub>H<sub>9</sub>OH might have been a contamination product from unrelated experimental samples that were being analyzed with GC-MS. Column backgrounds were determined by running the GC-MS method with no injection. Syringe backgrounds were determined by sampling 200 µL of room air and analyzing that injection with the set GC-MS method (Figure 3). Ultimately, the validity of the C<sub>4</sub>H<sub>9</sub>OH results could not be determined for these tests. Additional testing was not performed until other projects that cause potential interferences were completed.

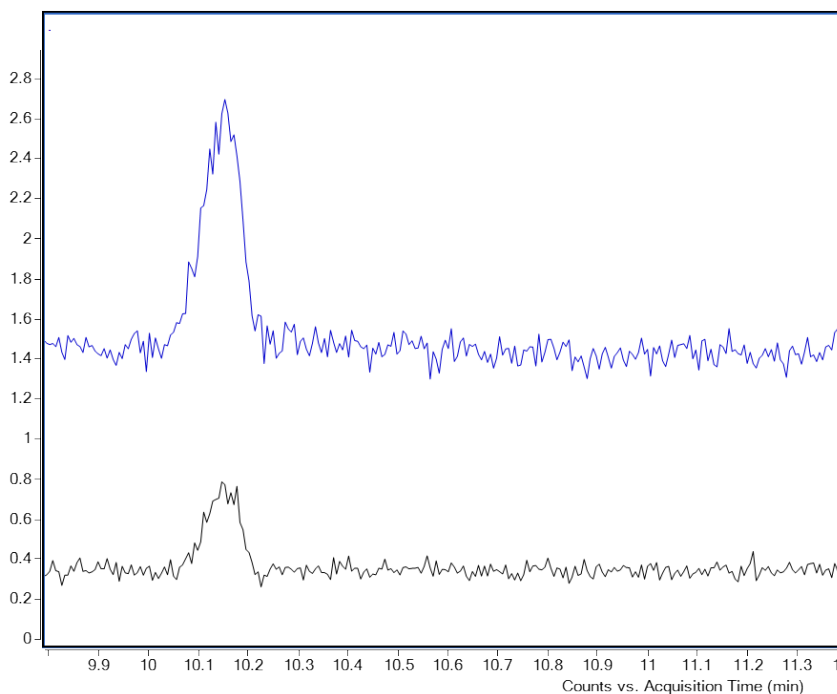


**Figure 3.** Chromatograph showing a syringe background sample (black, ~6 ppm) and an effluent sample from the humid SM-3 test (blue, ~12 ppm).  $C_4H_9OH$  (peak at 10 min) is present in both samples, suggesting that contamination from the syringe could account for  $C_4H_9OH$  signals observed in the effluents of SM-2 and SM-3.

## 4.2 SM-4 and SM-5: $C_4H_9I$ Thin Bed Tests

The goal of these tests was to determine whether  $C_4H_9OH$  was present in the test effluent. The tests were designed to run until a  $C_4H_9I$  breakthrough was observed. One thin bed test was run with a dry air stream at a dew point of  $-65^\circ C$ , and the second thin bed test was run under a humid air stream at a dew point of  $0^\circ C$ . Both tests used 18 g of AgZ (~1 in. deep) and a 50 ppm  $C_4H_9I$  inlet stream. The dry test (SM-4) ran for 30 h, and the humid test (SM-5) ran for 72 h. In the dry test, the inlet concentration was increased to 100 ppm after 24 h in an attempt to increase the concentration of any potential reaction products for easier detection. In the humid test, the concentration was held constant at 50 ppm for the 72 h test.

No  $C_4H_9OH$  or other reaction products were detected in the dry test under a 50 ppm stream or a 100 ppm stream. After 29 h,  $C_4H_9I$  breakthrough was observed.

Similarly, in the humid test, no  $C_4H_9OH$  was detected in any of the 10 effluent samples analyzed over 3 days.  $C_4H_9I$  breakthrough was detected in the effluent at 72 h.

## 4.3 SM-6 and SM-7: $C_4H_9I$ and $C_4H_9OH$ Burn-Off Tests

With no detection of  $C_4H_9OH$  in the effluents of SM-4 and SM-5, consideration was given to the potential that  $C_4H_9OH$  might be produced and subsequently be retained by the sorbent bed. The goal of tests SM-6 and SM-7 was to determine whether  $C_4H_9OH$  initially adsorbed to the AgZ during loading and could be removed at an elevated temperature. To test this possibility,  $C_4H_9OH$  was passed through a bed of AgZ at  $150^\circ C$  to establish any sorption. The  $C_4H_9OH$  flow was then discontinued, and the bed temperature was

increased to 225°C while effluent samples were collected. An C<sub>4</sub>H<sub>9</sub>I loaded test was sampled at the same temperature profile for comparison.

In test SM-6, a thin bed of AgZ (4 g total mass) was contacted with a humidified gas stream that contained 50 ppm C<sub>4</sub>H<sub>9</sub>I for 168 h (Table 3). Effluent samples were collected downstream of the thin bed repeatedly to measure the breakthrough concentration. Throughout the loading period, the mean downstream effluent C<sub>4</sub>H<sub>9</sub>I concentration was 41 ppm.

In test SM-7, a thin bed of AgZ (4 g total mass) was contacted with a dry gas stream that contained 50 ppm C<sub>4</sub>H<sub>9</sub>OH for 48 h (Table 3). Effluent samples were collected downstream of the thin bed during loading to measure the breakthrough concentration. Concentrations of 25 ppm were detected in the downstream effluent after 2 h, 43 ppm were detected downstream after 30 h, and 31 ppm were detected downstream after 48 h. This fluctuating concentration is not readily explained. The downstream concentrations are lower than the inlet concentration, suggesting that C<sub>4</sub>H<sub>9</sub>OH was being adsorbed to the AgZ during the loading phase.

After loading, the beds were purged with dry air at 150°C. Over the course of several hours, the bed temperature was increased to 160, 175, 200, and 225°C with effluent samples collected at each temperature (Table 4). The boiling point of C<sub>4</sub>H<sub>9</sub>OH is 117°C, which is well below the final temperature of the sorbent bed. Literature indicates that C<sub>4</sub>H<sub>9</sub>OH adsorbed on other similar zeolites will release at temperatures well below 200°C (Oudshoorn et al. 2012).

**Table 4.** Results of C<sub>4</sub>H<sub>9</sub>I and C<sub>4</sub>H<sub>9</sub>OH burn-off tests.

GC sample	Effluent sample	Temp. (°C)	C <sub>4</sub> H <sub>9</sub> OH (ppm)	C <sub>4</sub> H <sub>9</sub> I (ppm)
1	SM-6 C <sub>4</sub> H <sub>9</sub> I (loading)	150	BDL	46
2	SM-7 C <sub>4</sub> H <sub>9</sub> OH (loading)	150	31	--
Stop C <sub>4</sub> H <sub>9</sub> I flow, continue air diluent				
3	SM-6 C <sub>4</sub> H <sub>9</sub> I	150	BDL	21
Stop C <sub>4</sub> H <sub>9</sub> OH flow, continue air diluent				
4	SM-7 C <sub>4</sub> H <sub>9</sub> OH	150	3	--
Raise temperature to 160°C				
5	SM-6 C <sub>4</sub> H <sub>9</sub> I	160	BDL	16
6	SM-7 C <sub>4</sub> H <sub>9</sub> OH	160	BDL	--
Raise temperature to 175°C				
7	SM-6 C <sub>4</sub> H <sub>9</sub> I	175	BDL	14
8	SM-7 C <sub>4</sub> H <sub>9</sub> OH	175	BDL	--
Raise temperature to 200°C				
9	SM-6 C <sub>4</sub> H <sub>9</sub> I	200	BDL	BDL
10	SM-7 C <sub>4</sub> H <sub>9</sub> OH	200	BDL	--
Raise temperature to 225°C				
11	SM-6 C <sub>4</sub> H <sub>9</sub> I	225	BDL	BDL
12	SM-7 C <sub>4</sub> H <sub>9</sub> OH	225	BDL	--



## 4.4 SM-8: CH<sub>3</sub>I Loading and Burn-Off

One experiment was completed to determine whether CH<sub>3</sub>OH was detected during CH<sub>3</sub>I sorption on a thin bed of AgZ under humid conditions (Table 3). Fifty parts per million of CH<sub>3</sub>I in air was loaded on a thin bed of AgZ at 150°C and a dew point of 10°C. Loading was initiated at a dew point of 0°C but was raised to 10°C after several hours. After 2 days of loading, the CH<sub>3</sub>I flow was stopped, and air was purged through the bed as the temperature was raised in 25°C increments to 225°C. The effluent was sampled at each temperature increment.

During the loading portion of the test at 150°C, transient CH<sub>3</sub>OH was identified in effluent in the 10°C stream but not in the 0°C stream. The observed CH<sub>3</sub>OH was detected at the correct mass to charge ratio and retention time, but did not form a statistically significant peak (2σ above baseline) and could not be quantified.

During the loading portion of the test at 150°C, 50 ppm of CH<sub>3</sub>I was consistently detected downstream of the bed. That is, only a fraction of CH<sub>3</sub>I present in the feed stream was sorbing to the AgZ during the loading period. This would be expected in a thin bed test in which the concentration of sorbate is assumed to be nearly unchanged across the bed. In contrast, the SM-6 C<sub>4</sub>H<sub>9</sub>I thin bed test, which ran under similar conditions (150°C, 0°C dew point, identical flow rates, 4 g AgZ bed), recorded lower breakthrough concentrations with a mean of 41 ppm. This suggests that C<sub>4</sub>H<sub>9</sub>I sorbs onto AgZ differently than CH<sub>3</sub>I. These data support observations from TGA testing that show AgZ experiencing a faster initial weight gain and reaching saturation more quickly for C<sub>4</sub>H<sub>9</sub>I sorption than for CH<sub>3</sub>I sorption (Figure 4).

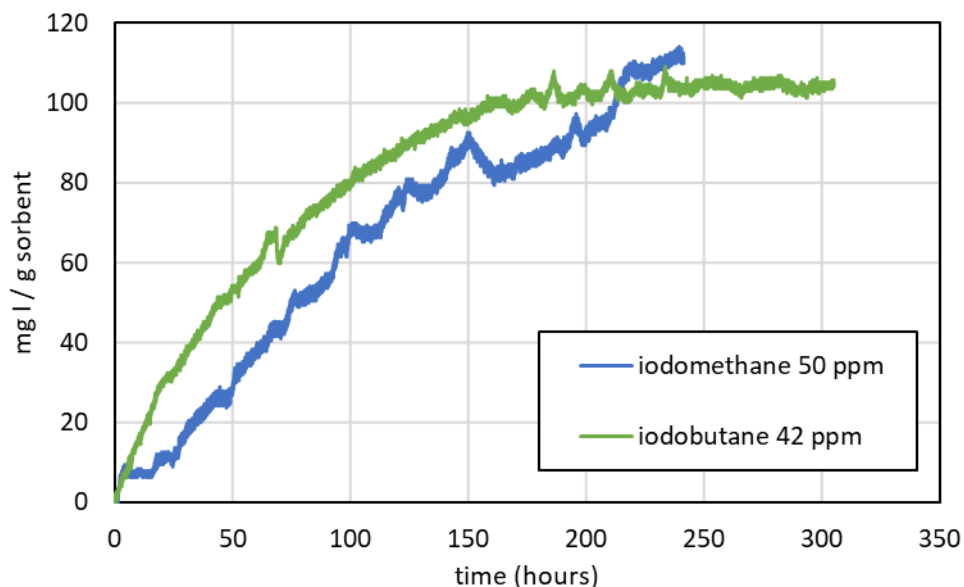


Figure 4. Loading rates of CH<sub>3</sub>I and C<sub>4</sub>H<sub>9</sub>I on thin bed tests recorded by TGA.

During the burn-off portion of the test, no CH<sub>3</sub>I or CH<sub>3</sub>OH was detected in the effluent stream. As soon as the CH<sub>3</sub>I loading flow was stopped, it disappeared from the effluent. This contrasts with the similar C<sub>4</sub>H<sub>9</sub>I test (SM-6) in which C<sub>4</sub>H<sub>9</sub>I was detected in the effluent stream for a few hours after the flow was stopped (between 150°C and 175°C) (Table 4). This observation could indicate higher levels of physisorption for C<sub>4</sub>H<sub>9</sub>I on AgZ compared with CH<sub>3</sub>I.

## 5. CONCLUSIONS AND FUTURE TESTS

Thin bed CH<sub>3</sub>I tests conducted at a 10°C dew point resulted in the identification of CH<sub>3</sub>OH in the chromatograph at levels near the LOD, confirming literature observations and the experimental methodology used in these studies. To bolster this observation, testing with greater masses of sorbent can be performed to increase the amount of sorbent available for reaction and the corresponding amount of CH<sub>3</sub>OH produced to well above the LOQ.

C<sub>4</sub>H<sub>9</sub>I and CH<sub>3</sub>I show different loading rates in TGA tests and thin bed tests in which the effluent is analyzed downstream of the test. C<sub>4</sub>H<sub>9</sub>I sorbs to AgZ more quickly than CH<sub>3</sub>I. C<sub>4</sub>H<sub>9</sub>I is also released from the sorbent during burn-off, whereas CH<sub>3</sub>I is not.

Thin bed C<sub>4</sub>H<sub>9</sub>I tests conducted at -65°C and a 0°C dew point did not result in C<sub>4</sub>H<sub>9</sub>OH detection in the effluent, strongly indicating that C<sub>4</sub>H<sub>9</sub>I sorption follows a different reaction pathway than CH<sub>3</sub>I sorption.

To finalize this experimental thrust before completing the comprehensive VOG testing program, select additional data will be collected. These actions will include: (1) determining the iodine content of each AgZ bed used in testing and (2) replicating SM-7 and SM-8 by using deep beds of AgZ to ensure that any CH<sub>3</sub>OH and C<sub>4</sub>H<sub>9</sub>OH produced are above the LOQ. These results will be included in the final end-of-year report.

## 6. REFERENCES

- Azambre, B. and M. Chebbi. 2017. "Evaluation of Silver Zeolites Sorbents Toward Their Ability to Promote Stable CH<sub>3</sub>I Storage as AgI Precipitates." *ACS Applied Materials & Interfaces* 9(30): 25,194–25,203.
- Bruffey, S. H., B. B. Spencer, D. M. Strachan, R. T. Jubin, N. R. Soelberg, and B. J. Riley. 2015. *A Literature Survey to Identify Potentially Problematic Volatile Iodine-Bearing Species Present in Off-Gas Streams*, FCR&D-MRWFD-2015-000421, ORNL-SPR-2015/290, INL/EXT-15-35609.
- Bruffey, S. H., R. T. Jubin, and J. A. Jordan. 2018. *Quantify the Extent of Physisorption on Silver Based Sorbents under VOG Conditions*, ORNL/SPR-2018/1066. Oak Ridge National Laboratory, Oak Ridge, Tennessee.
- Chapman, K. W., P. J. Chupas, and T. M. Nenoff. 2010. "Radioactive Iodine Capture in Silver-Containing Mordenites through Nanoscale Silver Iodide Formation." *Journal of the American Chemical Society* 132(26): 8,897–8,899.
- Chebbi, M., S. Chibani, J. F. Paul, L. Cantrel, and M. Badawi. 2017. "Evaluation of Volatile Iodine Trapping in Presence of Contaminants: A Periodic DFT Study on Cation Exchanged-Faujasite." *Microporous and Mesoporous Materials* 239: 111–122.
- Chebbi, M., B. Azambre, L. Cantrel, and A. Koch. 2016. "A Combined DRIFTS and DR-UV-Vis Spectroscopic In Situ Study on the Trapping of CH<sub>3</sub>I by Silver-Exchanged Faujasite Zeolite," *Journal of Physical Chemistry C* 120: 18,694–18,706.
- Greaney, A. T., and S. H. Bruffey. 2020. *Effect of NO<sub>x</sub> and Water Variations on Iodine Loading of AgZ*, ORNL/SPR-2021/1581, Oak Ridge National Laboratory, Oak Ridge, Tennessee.
- Haefner, D. R., and T. L. Watson. 2010. *Summary of FY2010 Iodine Capture Studies at the INL*, INL/EXT-10-19657.

- Huve, J., A. Ryzhikov, H. Nouali, V. Lalia, G. Augé, and T. J. Daou. 2018. “Porous Sorbents for the Capture of Radioactive Iodine Compounds: A Review.” *RSC Advances* 8(51): 29,248–29,273.
- Jubin, R. T., N. R. Soelberg, D. M. Strachan, and G. Ilas. 2012. *Fuel Age Impacts on Gaseous Fission Product Capture During Separations*, FCRD-SWF-2012-000089.
- Jubin, R. T., D. M. Strachan, and N. R. Soelberg. 2013. *Iodine Pathways and Off-Gas Stream Characteristics for Aqueous Reprocessing Plants—A Literature Survey and Assessment*, FCRD-SWF-2013-000308, ORNL/LTR-2013/383, INL/EXT-13-30119.
- Jubin, R. T., J. A. Jordan, and S. H. Bruffey. 2017. *Performance of Silver-Exchanged Mordenite and Silver-functionalized Silica-Aerogel under Vessel Off-gas Conditions*, ORNL/TM-2017/477, Oak Ridge National Laboratory, Oak Ridge, Tennessee.
- Jubin, R. T., S. H. Bruffey, N. R. Soelberg, and A. K. Welty. 2018. *Joint Test Plan for the Evaluation of Iodine Retention for Long-Chain Organic Iodides*, NTRD-MRWFD-2018-000212, ORNL/SPR-2018/781.
- Nenoff, T. M., M. A. Rodriguez, N. R. Soelberg, and K. W. Chapman. 2014. “Silver-Mordenite for Radiologic Gas Capture from Complex Streams: Dual Catalytic CH<sub>3</sub>I Decomposition and I Confinement.” *Microporous and Mesoporous Materials* 200: 297–303.
- Oudshoorn, A., L. A. M. Van der Wielen, and A. J. J. Straathof. 2012. “Desorption of Butanol from Zeolite Material.” *Biochemical Engineering Journal* 67: 167–172.
- Chebbi, M., B. Azambre, C. Monsanglant Louvet, B. Marcillaud, A. Roynette, and L. Cantrel. 2021. “Effects of Water Vapour and Temperature on the Retention of Radiotoxic CH<sub>3</sub>I by Silver Faujasite Zeolites.” *Journal of Hazardous Materials* 409: 124,947.
- Outotec, H. S. C. “Chemistry Software.” Version 9, 1974–2018.
- Scheele, R. D., L. L. Burger, and C. L. Matsuzaki. 1983. *Methyl Iodide Sorption by Reduced Silver Mordenite*, PNNL-4489.
- Soelberg, N. R., and T. L. Watson. 2016. *FY-2016 Methyl Iodide Higher NO<sub>x</sub> Adsorption Test Report*, INL/EXT-16-40087, Idaho National Laboratory, Idaho Falls, Idaho.
- Tang, S., S. Choi, Y. Nan, and L. L. Tavlarides. 2020. “Adsorption of Methyl Iodide on Reduced Silver-Functionalized Silica Aerogel: Kinetics and Modeling.” *AIChE Journal* e17137.